

Design of a custom power park for wind turbine system and analysis of the system performance under power quality disturbances

Sener Agalar, Yusuf Alper Kaplan ✉

Department of Electrical and Electronics Engineering, Anadolu University, Eskişehir, Turkey

✉ E-mail: yakaplan@anadolu.edu.tr

ISSN 1752-1416

Received on 28th November 2014

Revised on 28th April 2015

Accepted on 18th May 2015

doi: 10.1049/iet-rpg.2014.0412

www.ietdl.org

Abstract: This study presents an operation of custom power park (CPP) with wind turbine system (WTS). The classical power system stability, changes and challenges in the power system with installation of wind energy sources are given. The CPP is composed by static transfer switch (STS) for WTS. An electromagnetic transient model of a system is composed by WTS and STS in power system computer aided design/electromagnetic transient including DC (PSCAD/EMTDC) programme. The entire model of the proposed system is developed and simulating results are verified in PSCAD/EMTDC programme at different fault types. The system responses of the different fault types are given and obtained results are evaluated in detail for power quality problems. Moreover, of the different type faults are implemented to the WT feeder and the response of the proposed system is observed for all cases. Then, the simulating results are evaluated. The currents and voltages of all systems are investigated during normal, transfer and post-transfer periods and also these simulating results are evaluated.

1 Introduction

There is a strong rate of increase for wind energy installations in all developed countries. Due to the fact that wind energy has become such an important electric power source, stable operation also during grid disturbances is needed [1, 2]. Currently, wind energy is seen as a positive alternative to fossil fuels and also a way to assist the expansion of local economies in future. The world will use renewable energy instead of using fossil fuels in order to meet the demands of the world's energy. Energy planning and management are necessary to promote wind energy which has a vital importance for the development and future of all countries. Recent technological improvements on wind energy systems and the incentives provided by the governments have increased the penetration level of wind power into the grid. This phenomenon forces the transmission and distribution system operators to revise their grid codes. Moreover, these developments force the wind turbines stay connected to the grid during the disturbances in order to enhance system stability. This paper is devoted to the modelling of variable-speed wind turbines and the investigation of fault-ride through capability of wind turbines for grid integration studies [3]. The increasing use of sensitive loads makes it necessary to solve power quality (PQ) problems and to use custom power devices. This paper presents electromagnetic transient models of a system which is composed by wind turbine system (WTS) and static transfer switch (STS).

The main purpose of the proposed system is to supply specified PQ for customers, which includes an acceptable combination of following features:

- Power must be continuous.
- Duration and magnitude of the voltage reductions must be in specified limits.
- Duration and magnitude of the overvoltage must be in specified limits.

Until recently, voltage reductions and short-term outages were not an issue, the number of cumulative hours of interruptions per year

has been the benchmark measure for reliability has been changing, and the pace of change has accelerated. The basic aim of this paper is to develop simulation models of WTS. This paper deals with the modelling of custom power topologies for WTS in PSCAD/EMTDC. The related survey studies are presented under the following heads.

2 Improving the PQ with using STS

PQ of any system can be defined as having a bus voltage that closely resembles a sinusoidal waveform of required magnitude. The importance of PQ increases day-by-day because of increasing number of sensitive devices. Therefore losses are reduced and behaviours of interconnected networks are made more appropriate. Recently, PQ problems in the industry are increasing because PQ polluting loads are increasing day-by-day [4, 5]. The voltage quality is concerned with deviations of the voltage from the ideal. The ideal voltage is a sine wave of constant frequency and constant magnitude. The term voltage quality can be interpreted as the quality of the product delivered by the utility to the customers. Voltage and current are strongly related and if either voltage or current deviates from the ideal, it is hard for the other to be ideal. Voltage sag is a fundamental frequency decrease in the supply voltage for a short duration (five cycles to 1 min). Voltage swell is defined as the increase of fundamental frequency voltage for a short duration. An interruption occurs when the supply voltage (or load current) decreases to <0.1 per unit for a period of time not exceeding 1 min. When the supply voltage is zero for a period of time in excess of 1 min, the long duration voltage variation is called sustained interruption. The mentioned common voltage disturbances are shown in Fig. 1.

2.1 Impacts of wind farms on PQ

With the increasing share of wind energy sources and also because of other reasons discussed below, power systems are becoming less strong, that is, weak grid. There are many issues for PQ of wind farms in grid. Some of them are given in below:

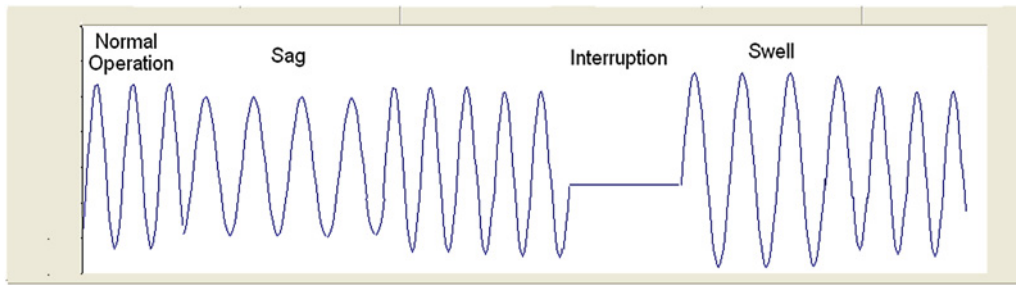


Fig. 1 Voltage disturbances

- Availability of the grid.
- Capacity of the grid.
- Reactive power.
- Voltage ranges.
- Voltage unbalance.
- Frequency range.
- Voltage fluctuations.
- Harmonics.

One of the most important issues of PQ is reactive power while grid availability, frequency range, voltage unbalance and voltage range are the primary parameters influencing the wind turbine operation [6, 7]. The new wind power plants are equipped with state-of-the-art technology in developed countries. Therefore they enable to supply good service generating clean and reliable power for grid. The many wind power system applications are more flexible thanks to advances in power electronics. Applications of PQ improvement, such as reactive power compensation, STS, energy storage and variable-speed generations are generally found in modern wind power plants [8].

2.2 STS operation

STSs are used to provide energy to a specific load with the highest possible quality by fast switching between two or more alternative power sources [9]. The STS contains two or more switches that allow transferring a load from a preferred feeder to a WTS, as in Fig. 2. STS is connected in the bus tie position when a sensitive load is supplied by two feeders. The STS is used in uninterruptible power supply systems and in distribution networks to provide connection to alternate sources of ac power for critical loads when WTS fails. The STS can be used very effectively to protect sensitive loads against voltage sags, swells and other electrical disturbances [10].

2.3 Control logic of STS

STS control system is composed of voltage-detection logic and a gating strategy. The detection logic is based on transforming ac voltages into a synchronously rotating frame. The gating system generates suitable gating patterns for the thyristor switches before, during and after a load transfer based on the direction of line current. Two different transfer schemes can be employed: zero-current strategy and commutation strategy. In zero-current strategy method of gating, load transfer to the back-up feeder is not performed until WTS transistors are turned off. When a disturbance is detected in the WTS, the gating signals are removed from WTS transistors. The gating logic will then wait for WTS transistors to be turned off which occurs after a current zero-crossing is reached. By applying zero-current gating scheme, a 'break-before-make' transfer can be achieved. However, the disadvantage of this system is the long transfer time. In commutation strategy method of gating, after a fault is detected, line current is compared against the zero-current threshold limit zero crossing transfer (ZCT). Depending on the direction of the line current, one of the alternate transistor switches is gated, for

example, if commutation occurs, the other leg of alternate transistor is also gated and the load-transfer process is over. Otherwise, the transfer will be postponed until commutation conditions are met. This happens if either voltage polarity or line current direction changes. This type of transfer is normally referred to as 'make-before-break' (MBB) transfer. To achieve a faster load transfer, commutation gating strategy can be employed. In this method of gating, the control system does not wait for the current zero-crossings and starts the transfer as soon as the disturbance is detected. Commutation gating strategy ('MBB') is used in the STS. The control circuit of the proposed system is responsible for monitoring the quality of the WTS voltages and performing a load transfer when any fault occurs. On the basis of abc-to-dq0 transformation, WTS line voltages are transformed into a synchronously rotating frame. This change of variables is through Park's transformation matrix

$$V_{dq0p} = K_s V_{abc} \quad (1)$$

where

$$\begin{pmatrix} V_{dq0p} \end{pmatrix}^T = \begin{bmatrix} V_{dp} & V_{qp} & V_{0p} \end{bmatrix} \quad (2)$$

$$\begin{pmatrix} V_{abc} \end{pmatrix}^T = \begin{bmatrix} V_{abp} & V_{bcp} & V_{cap} \end{bmatrix} \quad (3)$$

$$K_s = \frac{2}{3} \begin{bmatrix} \cos(\theta) & \cos(\theta - 120) & \cos(\theta + 120) \\ \sin(\theta) & \sin(\theta - 120) & \sin(\theta + 120) \\ 1/2 & 1/2 & 1/2 \end{bmatrix} \quad (4)$$

$$\theta(t) = \int_0^t \omega(\zeta) d\zeta + \theta(0) \quad (5)$$

where V_{abp} V_{bcp} V_{cap} are the preferred source line voltages, V_{dp} V_{qp} V_{0p} are dq0 components of the preferred source

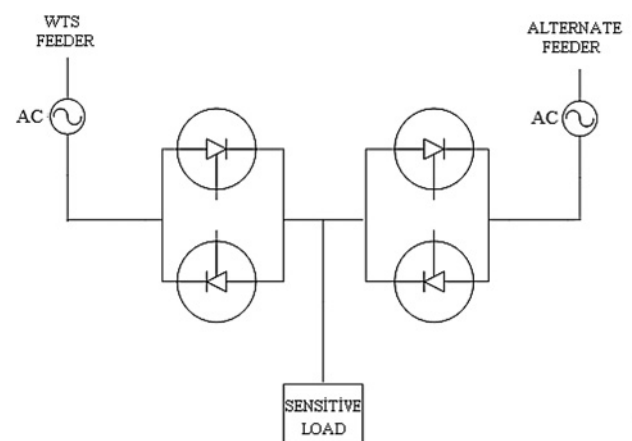


Fig. 2 Structure of an STS

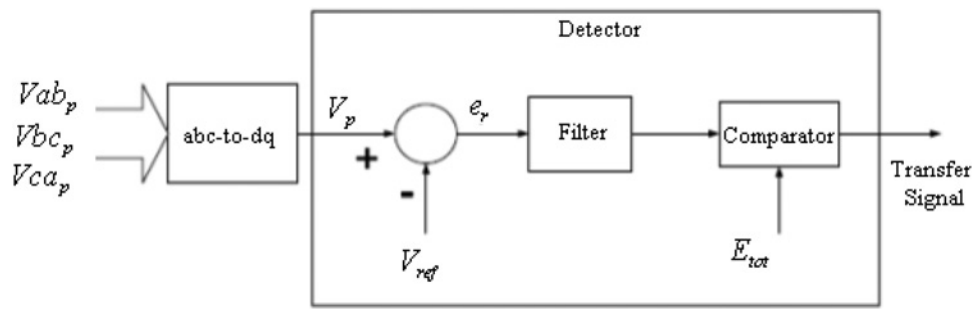


Fig. 3 Block diagram of the voltage-detection circuit

voltage in the rotating frame, K_s is the Park's transformation matrix, ω is the rotating frame angular frequency, θ is the rotation angle, $\theta(0)$ is the initial value of θ .

The root-mean-square value of V_{dp} and V_{qp} will then be calculated as

$$V_p = \sqrt{V_{dp}^2 + V_{qp}^2} \quad (6)$$

Fig. 3 shows that the output of the abc-to-dq0 transformation block, that is, the obtained dc value of V_p is compared with a dc reference, that is, V_{ref} . Then, the error signal is obtained and this signal is passed through a low-pass filter which attenuates impacts of voltage transients. The filter introduces a certain amount of delay to the error signal which is determined by the filter cut-off frequency (f_c). The output of the filter is compared with a tolerance limit E_{tot} which is determined before. Finally, the output of the comparator is the transfer-signal which initiates a transfer process of all systems if the preferred source fails. Two identical logics have been used for both sources [11, 12].

The PSCAD model of obtaining the reference signal is shown in Fig. 4. If any unsymmetrical fault occurs, the resulting voltage sag is unbalanced and contains both positive sequence and negative sequence components. The synchronous frame voltages V_{dp} and V_{qp} then have dc components and ripples. Voltage sags will certainly lead to the reduction of the positive sequence voltage component, which is used by the proposed STS controller to identify voltage sags. It is clearly seen in Fig. 4 that the error signal is compared with 0.1 (10% sag). If the error signal is bigger than 0.1, system start transfer. The detection time is shorter for a more severe fault. The response of the voltage-detection logic is mainly determined by the filter cut-off frequency f_c . The higher the f_c is, the faster the detection circuit and the shorter the detection time.

2.3.1 Transfer and gating strategies of STS: The STS operation is responsible for monitoring the quality of the WTS and performing the transfer of the load from the WTS to the alternate source and vice versa. The required input signals to the control circuit are the three-phase voltages from two sources and phase currents from the critical load. The outputs of the control system

are the gating patterns for the WTS and alternate source thyristor switches [11]:

- Thyristor-gating strategy, which is the removing the gating signals from thyristors of the WTS and triggering thyristors of the alternate source and vice versa.
- A fast commutation of WTS thyristor switches for three phase depends on the magnitude and relative position of the WTS instant phase voltage and line current.
- Fault/disturbance characteristics determine voltage difference between the WTS and alternate source.
- Fault/disturbance characteristics determine voltage drop across incoming and outgoing thyristors during the transfer process.
- The detection time is determined by voltage-detection logic [11].

The current-based thyristor-gating strategy of the STS is shown in Fig. 5. The status of each thyristor is detected by current direction zero-crossing detection logic which prevents the parallel operation of the two sources during the transfer process. The gating pattern generating logic is used to generate patterns for both WTS and alternate source thyristor switches (T1 and T2 switches). The line voltage to phase voltage conversion block and the zero voltage back-up transfer logic is used to transfer the load at zero-crossing of phase voltage if any change of current direction cannot be detected [11]. To achieve a fast load transfer, the control system of the STS employs a fast commutation gating strategy. This method of gating is obviously depicted in flowchart. In this gating method, the control system does not wait for the current zero-crossings and starts the transfer as soon as the disturbance is detected. However, to minimise the probability of source paralleling and cross-current, the transfer process begins according to the direction of line currents.

Transfer signals for phase A which are composed in PSCAD programmes is seen in Fig. 6. The proposed transfer strategy is based on a selective gating scheme during the transfer. The scheme is to transfer the load within the shortest possible time and prevent the sources from being paralleled during the transfer process. The transfer time is determined by the gating strategy, load type, fault type, fault instant and system configuration. The gating signals are obtained for all phases. Thyristor-gating generation system is a selective gating strategy which generates

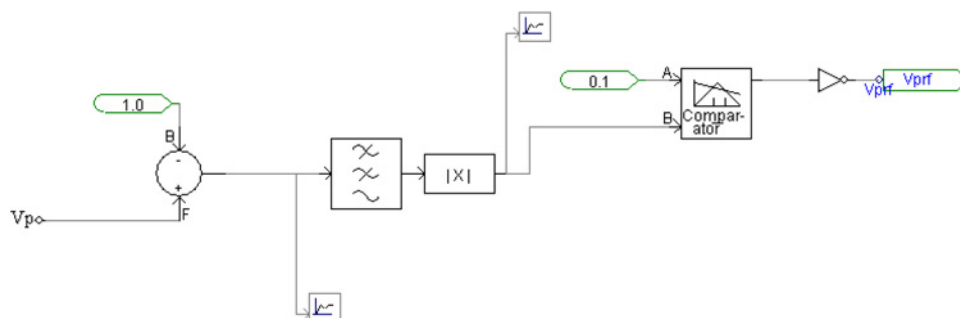


Fig. 4 V_{prf} signal in PSCAD/EMTDC

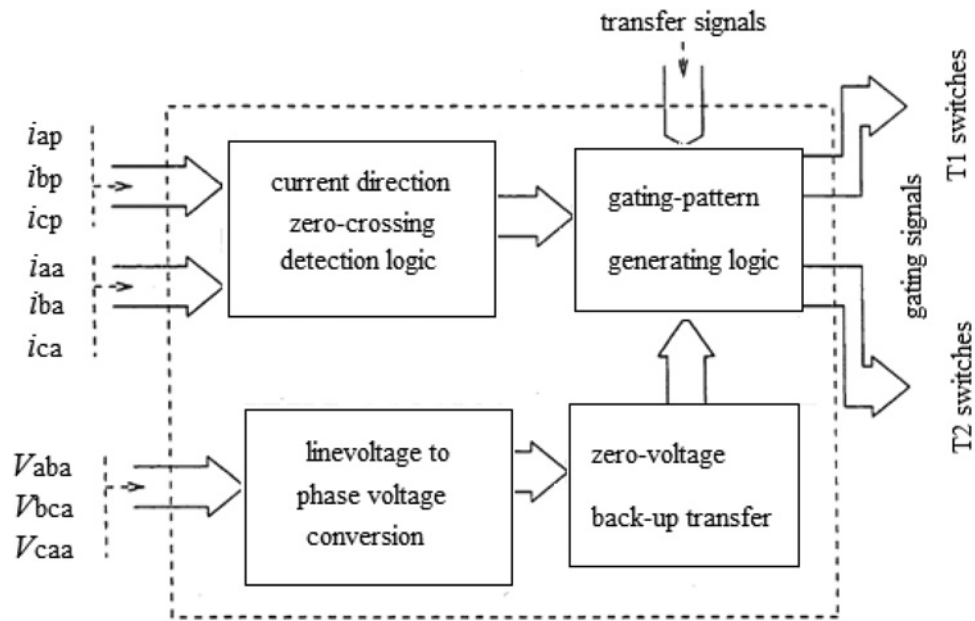


Fig. 5 Block diagram of thyristor-gating strategy

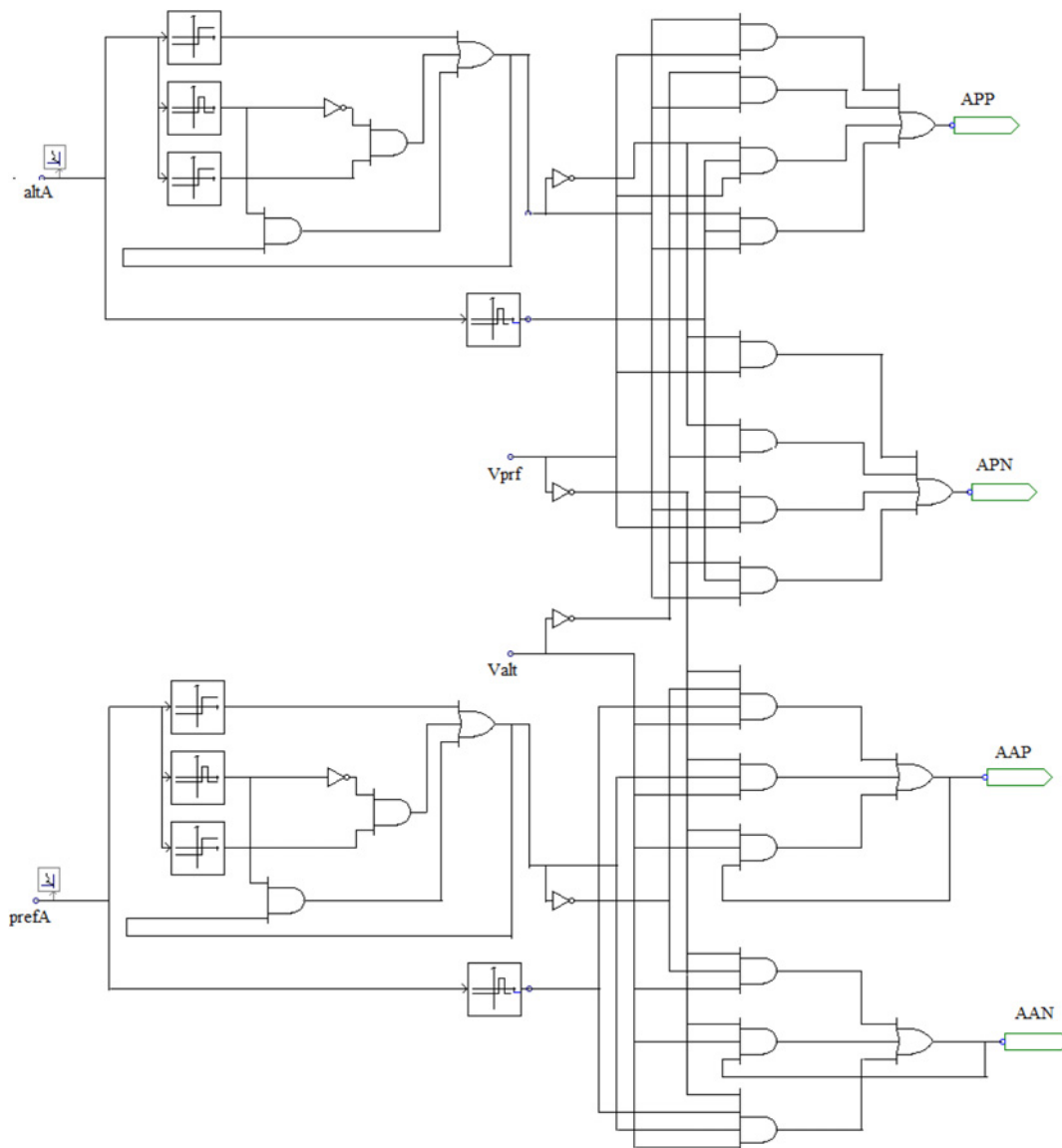


Fig. 6 Gating signals for one phase in PSCAD/EMTDC

gating signal for all phases during normal, transfer and post-transfer periods.

3 Wind turbine systems

Last technological improvements on wind energy systems and the incentives provided by the governments have increased the penetration level of wind power into the grid. This phenomenon forces the transmission and distribution system operators to revise their grid codes. Moreover, these developments force the wind turbines stay connected to the grid during the disturbances in order to enhance system stability [13]. Depleting fossil fuel reserves and the focus on sustainable development through the use of renewable energy sources have been the key motivators for the rapid development of wind energy conversion systems in the past couple of decades. Large wind turbine generators (WTGs) of the order of 2–6 MW have been developed and the units of 10 MW sizes are under development [14].

3.1 Wind turbine characteristics

In the wind turbine, wind energy can be efficiently captured by the variable-speed control. In a recent wind power generation, synchronous generator with the inverter system is almost adopted. The variable-speed control and the power factor control are executed in the wind power generation.

The kinetic energy of the air through the rotor blades is given by

$$E_{\text{wind}} = \frac{1}{2} \rho V v_w^2 \quad (7)$$

where ρ is the density of air (kilograms per cubic metres), V is the volume of air and V_w is the velocity of wind (metre per second (m/s))

$$P_{\text{wind}} = \frac{1}{2} \rho A_R v_w^3 = \frac{1}{2} \rho \pi R_r^2 v_w^3 \quad (8)$$

It is impossible to extract all the kinetic energy from the wind. The fraction of power harnessed by the wind turbine is given by its coefficient of performance, C_p . How this value is found is given below in detail

$$C_p = \frac{P_{\text{real}}}{P_{\text{th}}} \quad (9)$$

$$C_p = \frac{1}{2} (1 - a^2)(1 + a) \quad (10)$$

a is the tip-speed ratio which is the ratio of wind speed behind the rotor to wind speed in front of the rotor

$$P_{\text{mec}} = c_p(\lambda, \beta) \cdot P_{\text{wind}} \quad (11)$$

The power coefficient expression can be obtained from empirical expressions deduced from experimental tests or derived analytically from fluid dynamics theory applied to a certain turbine type, where $C_p(\lambda, \beta)$ is the power conversion coefficient expressed as a function of the blade pitch angle β and the tip-speed ratio λ . The tip-speed ratio is defined as

$$\lambda = \frac{W_r \cdot R_r}{V_w} \quad (12)$$

where R_r is the radius of the blade

$$C_p(\lambda, \beta) = 0.5 \left(\frac{116}{\lambda_i} - 0.4\beta - 5 \right) e^{-18.5/\lambda_i} \quad (13)$$

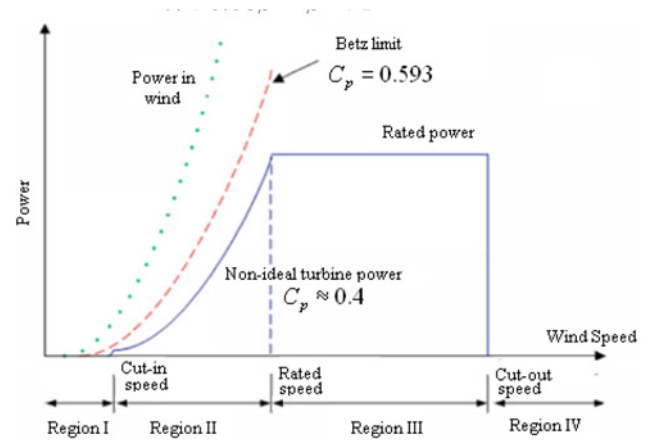


Fig. 7 Wind turbine characteristics

where

$$\lambda_i = \frac{1}{(1/(\lambda + 0.08\beta)) - (0.085/(\beta^3 + 1))} \quad (14)$$

Fig. 7 shows that totally different completely wind speed generates different power, when cut-out speed power goes to constant:

Region I: $V_{\text{wind}} < V_{\text{cut-in}}$, it means that turbine does not turn $P=0$.

Region II: Cut-in speed, the wind speed at that the turbine begins to obtain power for this system $V_{\text{cut-in}} = 4$ m/s.

Region III: Rated speed, the wind speed at that the wind turbine arrives at appraised turbine control. Ordinarily this could be frequently, nonetheless not consistently, the maximum power.

Region IV: Cut-out speed, the wind speed at that the turbine is pack up to stay masses and generator control from arriving at harming levels for this system $V_{\text{cut-out}} = 25$ m/s [15].

3.2 Wind turbine generators

A WTG comprises of a wind turbine for harnessing the kinetic energy of the wind into the mechanical energy of the rotating shaft which drives the generator. The mechanical energy is converted to electrical energy by the electrical generator. On the basis of rotational speed, in general, the WTG systems can be split into two types: fixed speed WTGS and variable-speed WTGS. Recently, three main types of wind turbines are used for generating of wind energy. These are the fixed speed wind turbine with squirrel cage induction generator, the variable-speed wind turbine with doubly fed induction generator and the variable-speed wind turbine with permanent magnet synchronous generator [16].

4 PSCAD model of WTS

In wind power stations, induction machines are often used as generators, but the development of new permanent magnet generators and its advantages for output PQ make other solutions possible [17]. A recent solution is to use a permanent magnet generator with variable speed and a conversion stage, which is the case studied in this technical study. We used the PSCAD/EMTDC programme to simulate the system. In PSCAD, the complete wind generator cycle is composed of:

- Wind source component.
- Wind turbine component.
- Wind governor.
- Synchronous generator.

This paper makes the choice to define a wind turbine connected to a permanent magnet synchronous generator with 100 pole pairs. The wind energy generating system (WEGS) is connected with grid having the sensitive load. We designed and simulated the WEGS which was generated combining STS and WTS to maintain PQ for sensitive loads. The proposed system which is designed in

PSCAD/EMTDC programme is shown in Fig. 8. There are two feeders: first one is wind turbine feeder the other one is alternate feeder. WT feeder is connected to Transformer P and alternate feeder is connected to Transformer A. Then these transformers are connected to thyristors. The outputs of the thyristors are connected to step down transformer and then the output of the transformer

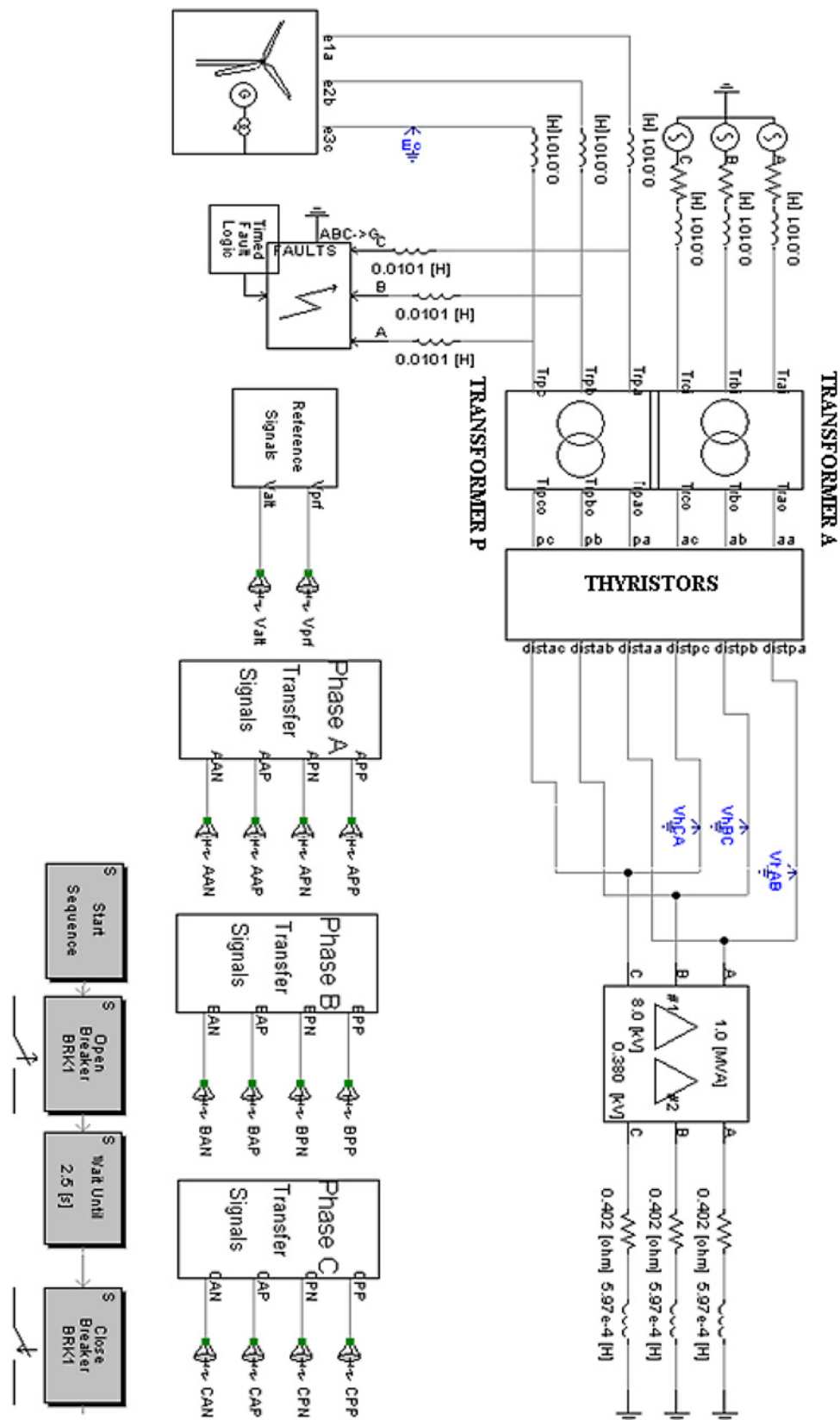


Fig. 8 STS and WTS implemented in PSCAD/EMTDC

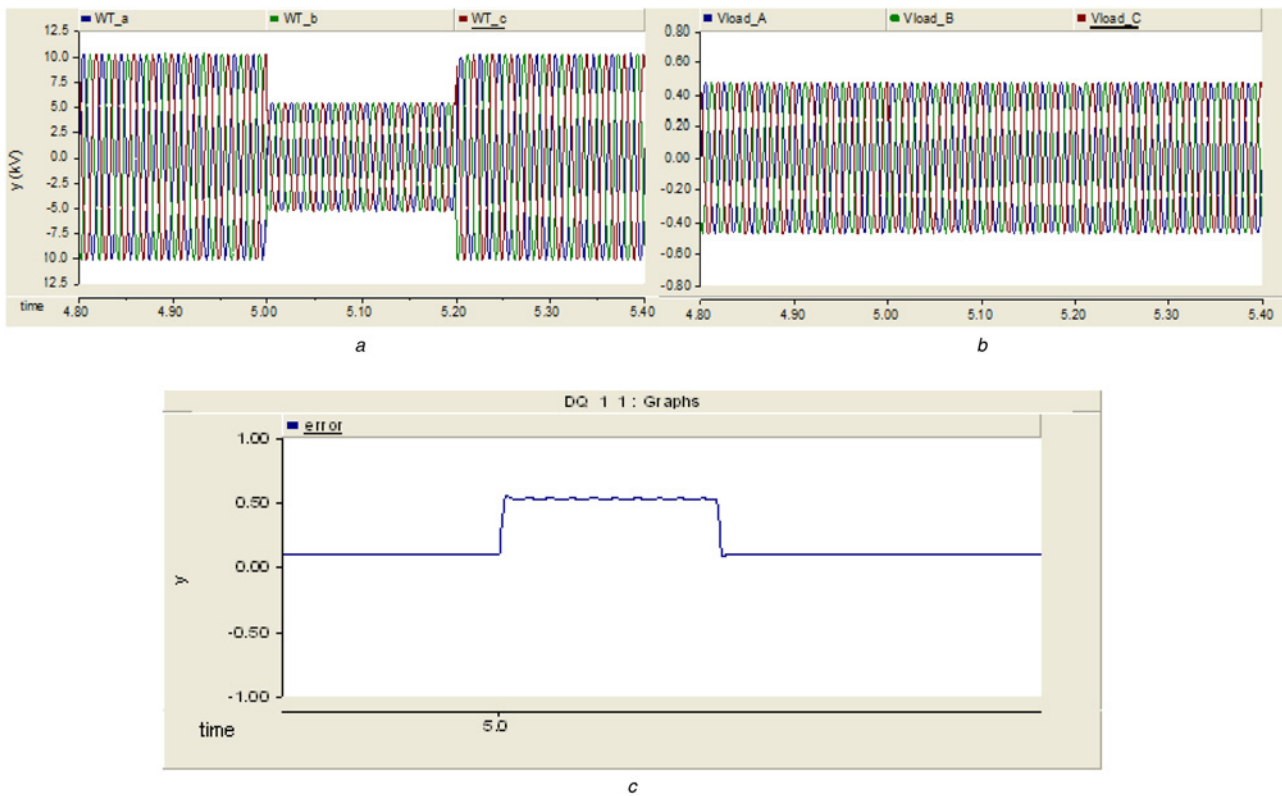


Fig. 9 Case 1: Under three-phase balanced fault

- a WTS source voltages at three-phase balanced fault
- b Load voltages at three-phase balanced fault
- c Error signal at three-phase balanced fault

connected to the sensitive load. Fault unit is connected to WTS to observe the response of the proposed system at fault duration. The all obtained simulating results are evaluated, comprehensively. The main purpose of the system is uninterrupted energy for sensitive loads. The transfer signals of thyristors are obtained for all phases from three different units which are shown in Fig. 8. We used breaker operation sequencers to improve starting conditions. To evaluate the performance of the proposed system, many electrical disturbances are implemented to the system. The system is modelled for different fault cases: interruption, voltage sag and voltage swell conditions.

The parameters of the proposed system are as follows:
WTS and alternate source systems

13.8 kV (line-to-line), 50 Hz

$$R_{WTS} = R_a = 0.015 \text{ W}, \quad X_{WTS} = X_a = 0.0101 \text{ H}$$

Transmission line

8 kV/100 kV, 250 MVA, 50 Hz Y/Δ step up transformer
100 kV/8 kV, 250 MVA, 50 Hz Δ/Y step down transformer

Three-phase Δ/Δ load transformer

8 kV/380 V, 1 MVA, 50 Hz

Each pair of thyristor valves has a snubber circuit composed of $R = 1 \text{ M}\Omega$ and $C = 0.001 \text{ }\mu\text{F}$.

Load system is composed of a three-phase load. The series load has the following parameters

$$R_L = 0.402 \text{ }\Omega, \quad X_L = 0.597 \text{ mH}$$

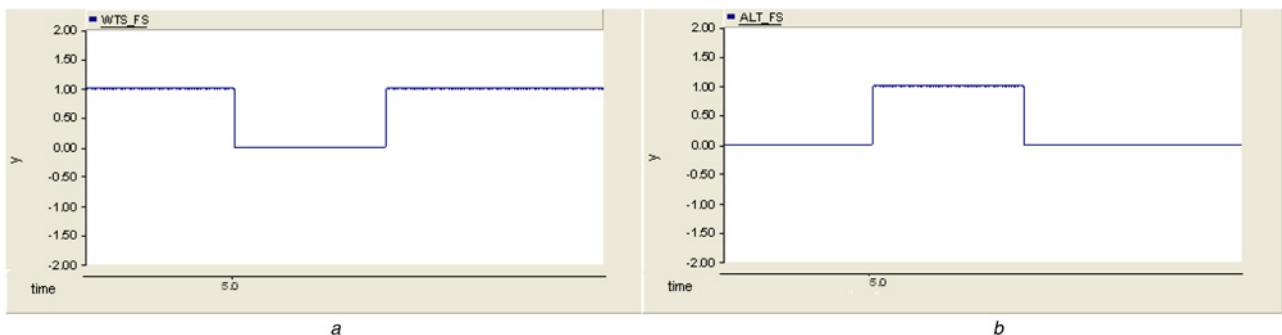


Fig. 10 Fault begins at time 5 s

- a WTS firing signal at three-phase balanced fault
- b Alternate feeder (AF) firing signal at three-phase balanced fault

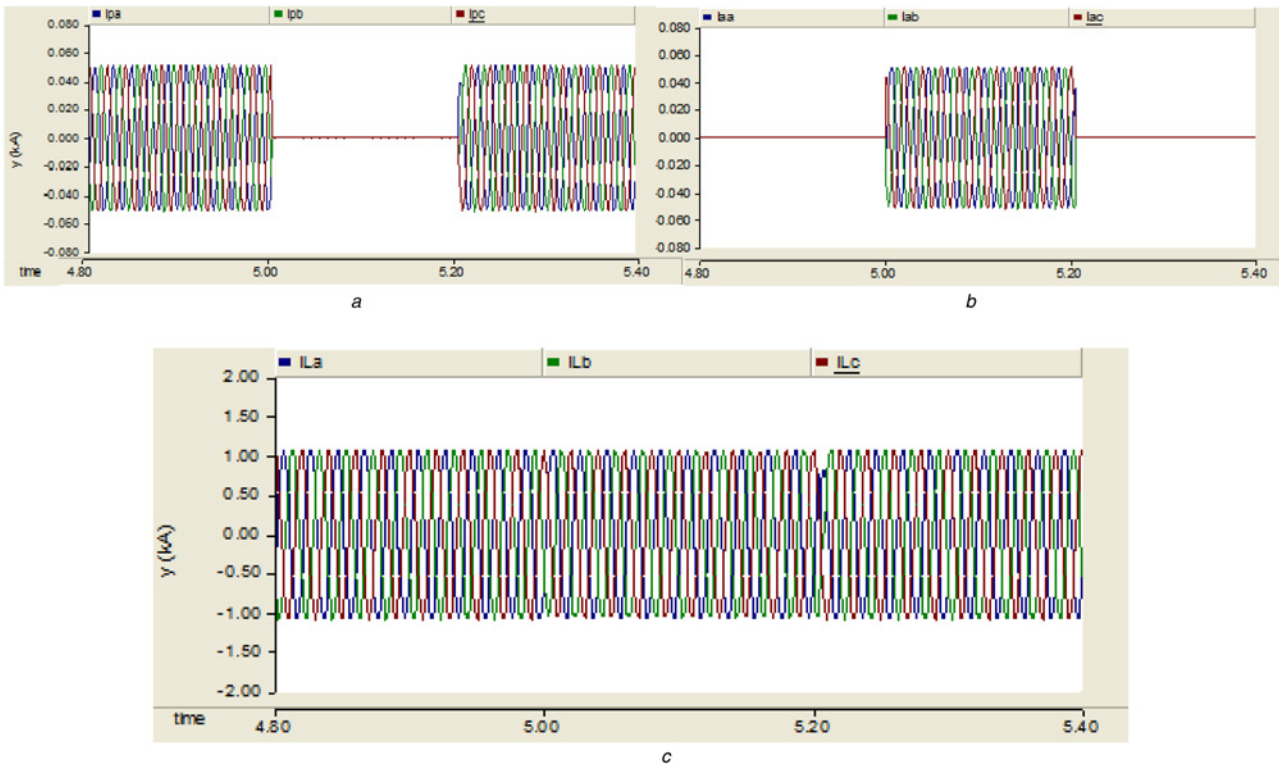


Fig. 11 Simulating current results at three-phase fault duration

- a WTS source current at three-phase balanced fault
- b Alternate source current at three-phase balanced fault
- c Load currents at three-phase balanced fault

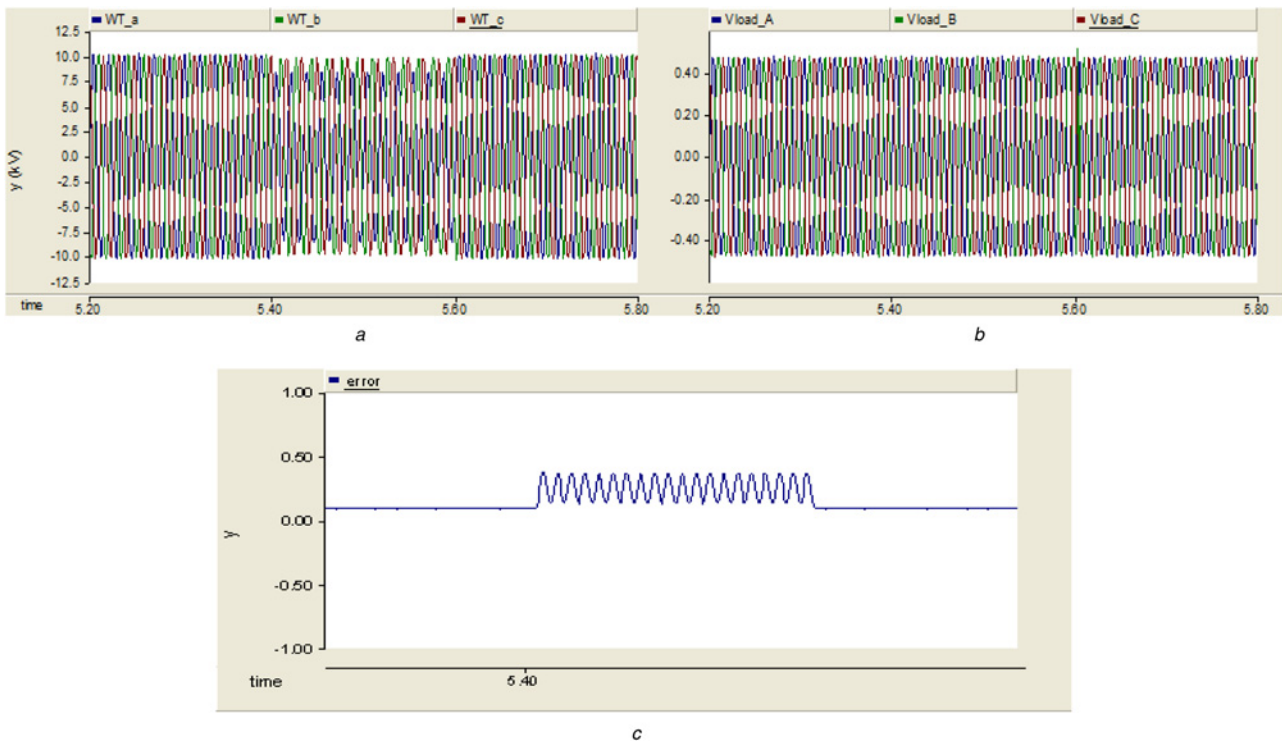


Fig. 12 Case 2: Under single phase-to-ground fault

- a WTS voltages at single phase-to-ground fault
- b Load voltages at single phase-to-ground fault
- c Error signal at single phase-to-ground fault

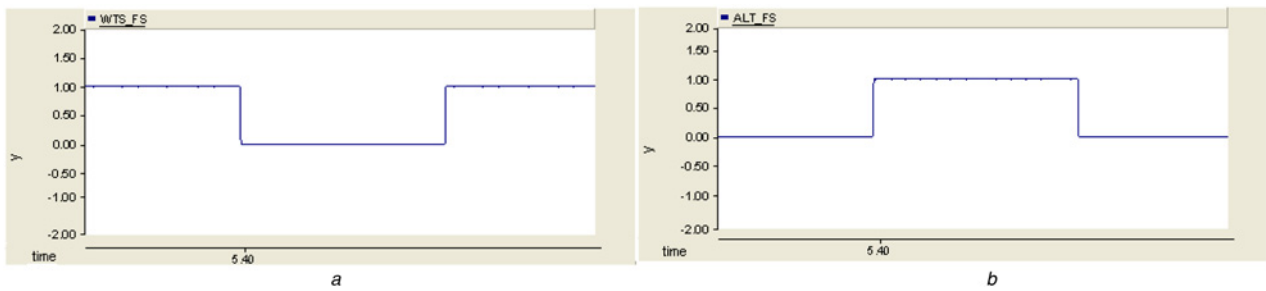


Fig. 13 Fault begins at time 5.4 s
a WTS firing signal at single phase-to-ground fault
b AF firing signal at single phase-to-ground fault

Control circuit parameters

$$\text{Voltage-change tolerance limit } E_{\text{tot}} = 10\% V_{\text{ref}}$$

5 Simulating results of the proposed system

Main motivation of this paper is to develop new control strategies for wind turbines' fault response that can enable increased wind power penetration in existing power systems without degrading the stability. As discussed above and in the literature, risks for security of a stable power system arise with high penetration of wind power, mainly because of distinct characteristics of wind power installations. In this paper, the purpose of making the WPPs behave similar to custom power parks (CPPs) is targeted, focusing on the response of WPPs during different grid faults. And also during interruption, voltage sag and swell condition the PQ of the sensitive load is maintained by STS. The modern wind turbines are equipped with the capability to stay connected and to support the grid during faults. The ability to support the grid during deep voltage transients caused by network disturbances depends on both the technical features and load of the connected generator, and the

dynamic characteristics of the grid [18]. In this paper, the purpose of making the WPPs behave similar to CPPs is targeted, focusing on the response of WPPs during different grid faults. And also during interruption, voltage sag and swell condition the PQ of the sensitive load is maintained by STS.

5.1 Case studies of fault conditions

Different types of faults are implemented to the WT feeder and the response of the proposed system is observed for all cases. Then, the simulating results are evaluated.

5.1.1 Case 1: under three-phase balanced fault: The fault occurs at $t_1 = 5$ s and detected at $t_2 = 5.2$ s. Figs. 9*a* and *b* show the WTS source voltage and the load voltages at three-phase fault duration. The total simulation duration of the system is 0.6 s. Since symmetrical fault occurs, V_p is calculated which is a dc value. Fig. 9*c* shows the error signal which is passed through a low-pass filter has a cut-off frequency 50 Hz. The filter attenuates impacts of voltage transients and introduces a certain amount of delay to the error signal which is determined by the filter cut-off

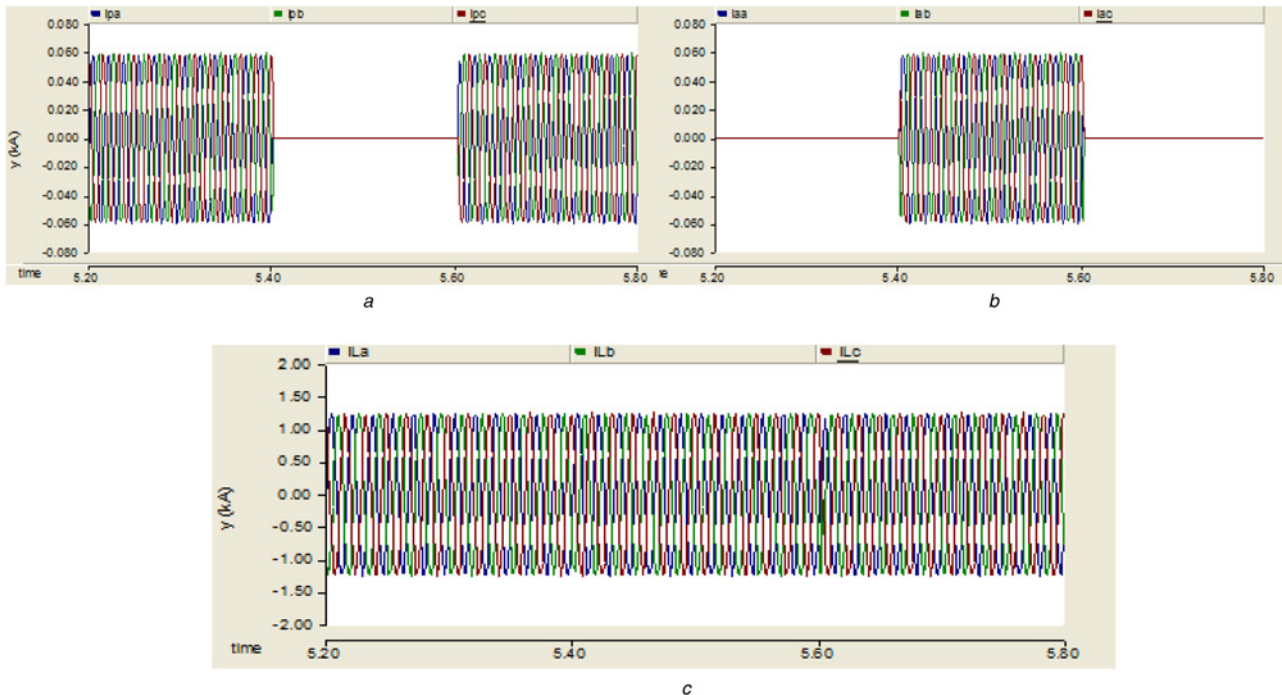


Fig. 14 Simulating current results at single phase-to-ground fault duration
a WTS source current at single-phase fault
b Alternate source current at single-phase fault
c Load currents at single-phase fault

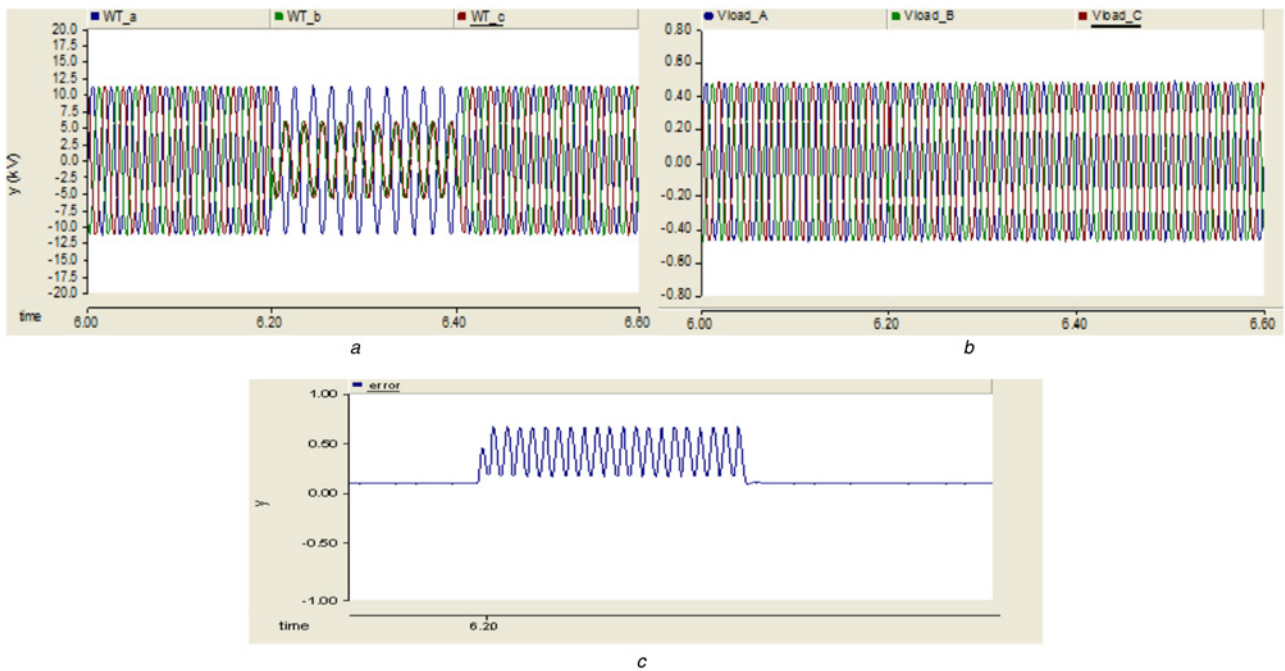


Fig. 15 Case 3: Under phase-to-phase fault

- a WTS voltages at single phase-to-phase fault
- b Load voltages at single phase-to-phase fault
- c Error signal at phase-to-phase fault

frequency. If the error signal is bigger than 0.1 (10% sag), system start transfer. Moreover, does not transfer back before the error signal is <0.02 ($98\% V_{ref}$) which is controlled by a hysteresis comparator (relay). Thyristor turn-off time is 1 ms and the transfer time is smaller than 5 ms.

Figs. 10a and b show that the fault begins at time 5 s and the gates positions of two feeders have been observed during the period from 4.8 to 5.4 s. Wind Tr signal is on and Valt Tr signal is off at fault duration after fault Wind Tr signal is on and Valt Tr signal is off.

Fig. 11 shows the simulating current results at three-phase fault duration. Fig. 11a shows the WTS currents measured from high side of the source transformer. Similarly, Fig. 11b shows the alternate source currents and Fig. 11c shows the load current which was measured the low-voltage side of load transformer.

5.1.2 Case 2: under single phase-to-ground fault: The single-phase fault is implemented to phase A. The fault occurs at $t_1 = 5.4$ s and detected at $t_2 = 5.6$ s. Figs. 12a and b show the WTS source voltage and the load voltages at single phase-to-ground fault duration. The total simulation duration of the system is 0.6 s. It is clearly seen in Fig. 12c that without fault conditions the value of the error signal is about zero. Since single phase-to-ground fault occurs, error signal is calculated. If the error signal is bigger than

0.1 (10% sag), system starts transfer. Transfer back to WTS source occurs when the error signal is <0.02 ($98\% V_{ref}$). Thyristor turn-off time is 1 ms and the transfer time is smaller than 5 ms.

Figs. 13a and b show that the fault begins at time 5.4 s and the gates positions of two feeders have been observed during the period from 5.2 to 5.8 s. Wind Tr signal is on and Valt Tr signal is off at fault duration after fault Wind Tr signal is on and Valt Tr signal is off.

Fig. 14 shows the simulating current results at single phase-to-ground fault duration. Fig. 14a shows the WTS currents measured from high side of the source transformer. Similarly, Fig. 14b shows the alternate source currents and Fig. 14c shows the load current which was measured the low-voltage side of load transformer.

5.1.3 Case 3: Under phase-to-phase fault: The phase-to-phase fault which is implemented between phase B and phase C occurs at $t_1 = 6.2$ s and detected at $t_2 = 6.4$ s. Figs. 15a and b show the WTS source voltage and the load voltages at phase-to-phase fault duration. The total simulation duration of the system is 0.6 s. Fig. 15c shows the magnitude of the error signal which is passed through a low-pass filter. The voltage sag is unbalanced and contains both positive sequence and negative

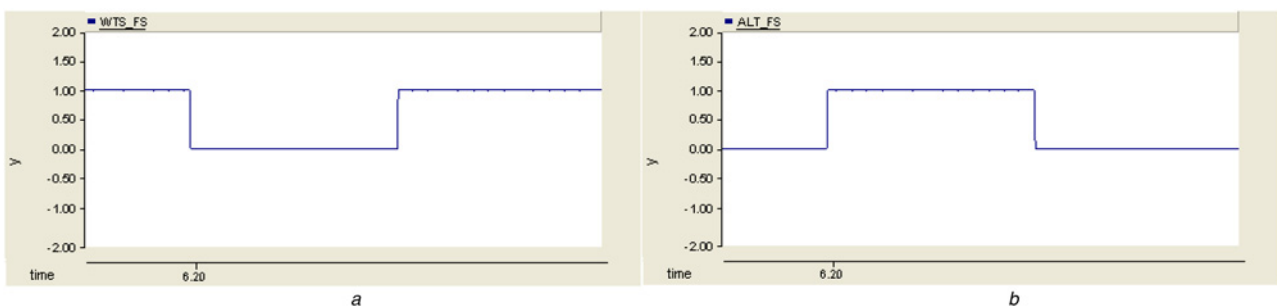


Fig. 16 Fault begins at time 6.2 s

- a WTS firing signal at phase-to-phase fault
- b AF firing signal at phase-to-phase fault

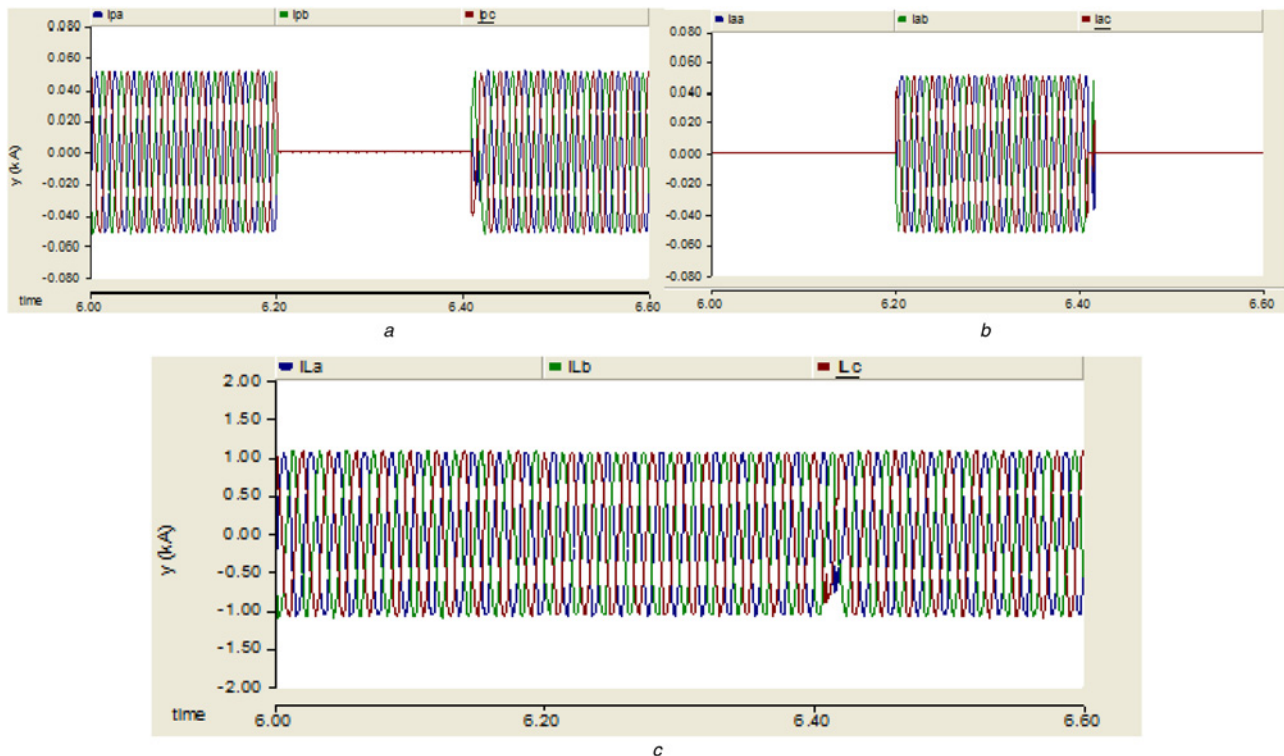


Fig. 17 Simulating current results at single phase-to-phase fault duration

a WTS source current at phase-to-phase fault
 b Alternate source current at single-phase fault
 c Load currents at single-phase fault

sequence components. It is seen that alternate feeder does not transfer back before the error signal is <0.02 ($98\% V_{ref}$). Thyristor turn-off time is 1 ms and the transfer time is smaller than 5 ms.

Figs. 16a and b show that the fault begins at time 6.2 s and the gates positions of two feeders have been observed during the period from 6 to 6.6 s. Wind Tr signal is on and Valt Tr signal is off at fault duration after fault Wind Tr signal is on and Valt Tr signal is off.

Fig. 17 shows the simulating current results at single phase-to-phase fault duration. Fig. 17a shows the WTS currents measured from high side of the source transformer. Similarly, Fig. 17b shows the alternate source currents and Fig. 17c shows the load current which was measured the low-voltage side of load transformer.

6 Conclusions

In this paper, the importance of sustainable, reliable and good quality power which is provided by utilities are emphasised. The main differences and importance of contributions of this paper can be summarised as follows: nowadays, to supply an uninterrupted and quality power is a very important issue for using wind energy in the electrical grid. In this paper, a wind turbine has been designed which is connected to network with STS. Thus the electrical network has been made safer and reliable to increase the use of wind turbines for generating electrical power. The new method is presented for the power generation of wind turbines. In the literature; theoretically, there has been reported not much work on the proposed system, design procedure and experimental analysis. This paper will also contribute to the concept finding solutions to the electric PQ problems of WTS. The performance of the proposed system is simulated for different faults/disturbance scenarios using the PSCAD programme. It can be seen from the simulating results of the proposed system that the system has fast dynamic response and good steady-state performance.

7 References

- Bongiorno, M., Thiringer, T.: 'Generic DFIG model for voltage dip ride-through analysis', *IEEE Trans. Energy Convers.*, 2013, **28**, (1), pp. 76–85
- GWEC (Global Wind Energy Council) – Global Wind 2013 Report, 2013
- Koç, E., Guven, A.: 'Modeling and investigation of fault ride through capability of variable speed wind turbines', *EMO Sci. J.*, 2011, **1**, (1), pp. 51–55
- Teke, A., Saribulut, L., Tumay, M.: 'Power quality disturbances and custom power devices', *C.U. J. Fac. Eng. Arch.*, 2011, **26**, (1), pp. 57–65
- Dong, Z.Y., Saha, T.: 'Power quality & equipment protection'. ELEC4301, 2004, pp. 1–34
- Hazim, F.B.: 'Design and implementation of a current source converter based STATCOM for reactive power compensation' (The Graduate School of Natural and Applied Sciences of Middle East Technical University, Ankara, Turkey, 2007)
- Li, H., Chen, Z.: 'Overview of different wind generator systems and their comparisons', *Renew. Power Gener.*, 2008, **2**, pp. 123–138
- Muljadi, E., Butterfield, C.P., Chacon, J., Romanowitz, H.: 'Power quality aspects in a wind power plant'. Proc. IEEE Power Engineering Society General Meeting, 2006
- Mahmood, T., Choudhry, M.A.: 'Application of static transfer switch for feeder reconfiguration to improve voltage at critical locations'. Transmission & Distribution Conf. and Exposition, Caracas, 2006, pp. 1–6
- Rauch, G.B., Shew, F., Horner, J.: 'Application of power quality recording instruments for monitoring medium voltage static transfer switch operation'. IEEE Power Engineering Society Summer Meeting, 1999, vol. 1, pp. 420–425
- Mokhtari, H., Dewan, S.B., Irvani, M.R.: 'Analysis of a static transfer switch with respect to transfer time', *IEEE Trans. Power Deliv.*, 2002, **17**, (1), pp. 190–199
- Sannino, A.: 'Static transfer switch: analysis of switching conditions and actual transfer time'. Power Engineering Society Winter Meeting, Columbus, 2001, vol. 1, pp. 120–125
- Zhu, W., Cao, R.: 'Improved low voltage ride-through of wind farm using STATCOM and pitch control'. IEEE Power Electronics and Motion Control Conf., IPEMC '09, Wuhan, 2009, pp. 2217–2221
- Liserre, M., Cardenas, R., Molinas, M., Rodriguez, J.: 'Overview of multi-MW wind turbines and wind parks', *IEEE Trans. Ind. Electron.*, 2011, **58**, pp. 1081–1095
- Bhandare, A.M., Jadhav, K., Ghat, M.B.: 'Performance of power coefficient & power with respect to variable wind speed'. IEEE Energy Efficient Technologies for Sustainability (ICEETS), Nagercoil, 2013, pp. 466–471
- Kadam, D., Kushare, B.E.: 'Overview of different wind generator systems and their comparisons', *Int. J. Eng. Sci. Adv. Technol. [IJESAT]*, 2012, **2**, (4), pp. 1076–1081
- Kenneth, E.O.: 'Wind turbine driven by permanent magnet synchronous generator', *Pac. J. Sci. Technol.*, 2011, **12**, (2), pp. 168–175
- Chowdhury, M.M., Haque, M.E., Gargoom, A., Negnevitsky, M.: 'Performance improvement of a grid connected direct drive wind turbine using super-capacitor energy storage' (Innovative Smart Grid Technologies (ISGT), Washington, 2013), pp. 1–6